Investigating ΔR_1 and ΔR_2* as Biomarkers of Tumour Oxygenation

J. S. Burrell[1], J. Halliday[2], S. Walker-Samuel[3], J. C. Waterton[2], J. Boult[1], Y. Jamin[1], L. C. Baker[1], and S. P. Robinson[1]
[1]The Institute of Cancer Research, Sutton, Surrey, United Kingdom, [2]AstraZeneca, Manchester, United Kingdom, [3]UCL, London, United Kingdom

Introduction: Tumour hypoxia is associated with aggressive, malignant phenotypes and is a major determinant of treatment response and patient outcome. A range of imaging methods are being investigated that may provide a means of assessing tumour hypoxia *in vivo* [1]. Molecular oxygen is paramagnetic, and therefore in solution shortens the MR longitudinal relaxation time T_1 of surrounding water protons [2]. *In vivo*, the level of molecular oxygen dissolved in blood plasma has been shown to cause tissue T_1 to change proportionally to the variation in O_2 concentration [3]. Controlled perturbation of blood plasma O_2 through breathing a hyperoxic gas mixture such as carbogen (95% O_2, 5% CO_2) results in a reduction in T_1 (ΔT_1), providing information about changes in tissue oxygenation status. ΔT_1 has therefore been proposed as a novel imaging biomarker of tissue and tumour oxygenation [3, 4]. This approach is distinct to intrinsic susceptibility MRI, which relies on the dependence of the tissue transverse relaxation rate R_2* on the ratio of oxy- to deoxyhaemoglobin in blood. Baseline R_2* and carbogen-induced ΔR_2* are also being investigated for the provision of imaging biomarkers of tumour hypoxia [5, 6]. Given the dependence of both T_1 and R_2* on blood oxygenation, we hypothesised that parallel use of the two biomarkers may provide a more informative index of tumour oxygenation than either does individually. To this end, changes in oxygenation in GH3 prolactinomas during carbogen breathing was investigated using ΔR_1 ($1/T_1$) and ΔR_2*.

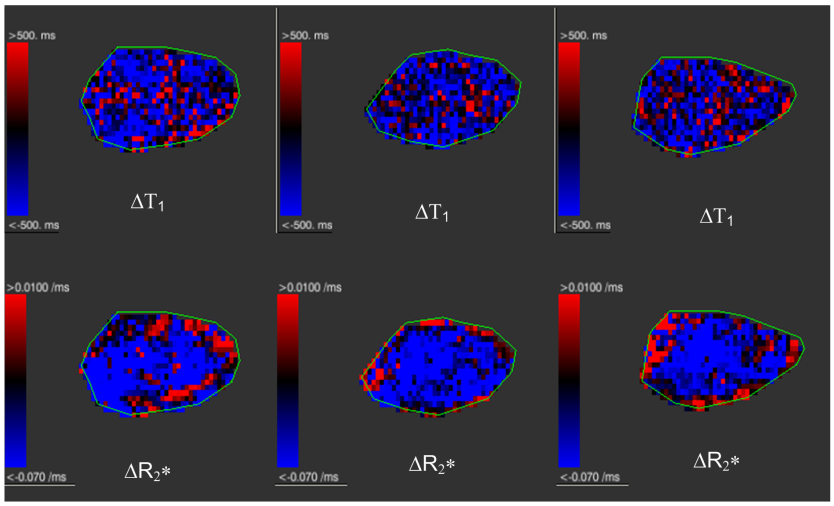

Figure 1. Representative maps of ΔT_1 and ΔR_2* from one GH3 prolactinoma

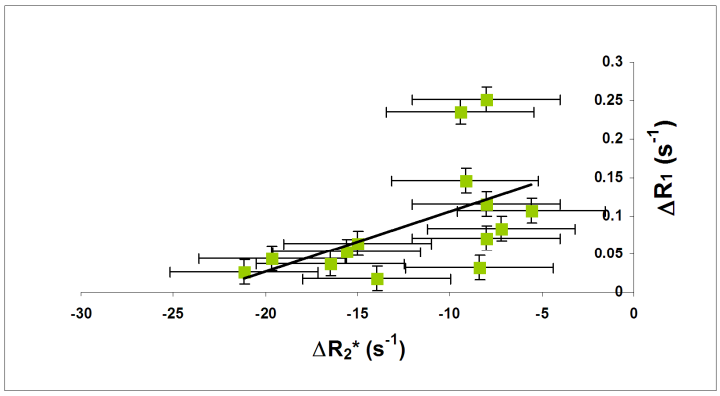

Figure 2. ΔR_2* plotted against ΔR_1 for each of three slices acquired from the six GH3 prolactinomas.

Baseline R_2* (s^{-1})	ΔR_2* (s^{-1})	Baseline R_1 (s^{-1})	ΔR_1 (s^{-1})
118.6 (±4)	-20.2 (±4)	0.61 (±0.02)	0.083 (±0.02)

Methods: GH3 prolactinomas were propagated by subcutaneous injection of 2.5×10^6 cells into the flanks of six female NCr nude mice. The tumours were imaged at a diameter of approximately 1cm. All images were acquired on a 7T horizontal bore Bruker system using a 3cm birdcage coil. The mice were anaesthetised and restrained using dental paste in order to limit motion artefacts [8]. A nosepiece was positioned for delivery of air or carbogen. TurboRARE images were acquired for tumour delineation, followed by two sets of baseline multi gradient echo (MGE) images (TR=200msec, TE=6–28ms, 4ms echo spacing, 8 averages, 2min 30s AQ), and one set of inversion recovery TrueFISP images (TE=1.2ms, TR=2.4ms, scan TR=10s, α=60°, 20 averages, 8 min AQ) from 3 contiguous 1mm slices acquired from a 3x3cm FOV and 128x128 matrix whilst the host breathed air. The gas supply was then switched to carbogen, and following a two minute transition time, further identical MGE and TrueFISP image sets acquired. **Data Analysis:** Data were fitted using a Bayesian maximum *a posteriori* approach. This approach takes into account the data's Rician noise distribution, which was used in the calculation of a log-likelihood function which incorporated the Rice probability density function [9]. Tumour T_1 and R_2* values were estimated on a pixel-by-pixel basis. The MGE signal magnitude was modelled as a single exponential decay, enabling estimates of ΔR_2* uncertainty ($\sigma_{\Delta R2^*}$) to be defined and the probability that a given ΔR_2* estimate was significantly greater than or less than zero.

Results and Discussion: Representative ΔT_1 and ΔR_2* maps from one GH3 tumour are shown in Figure 1. The ΔT_1 and ΔR_2* response to carbogen were independently spatially heterogeneous. Carbogen breathing significantly increased R_1 ($p=0.02$) and reduced R_2* ($p<0.05$) in all six tumours (see Table). The positive median ΔR_1 is consistent with an increase in dissolved plasma O_2 concentration. The reduction in R_2* indicates increased blood oxyhaemoglobin concentration.

A weak yet statistically significant correlation ($r=0.54$, $p<0.05$) was determined between ΔR_1 and ΔR_2* (Figure 2). This correlation suggests that tumours exhibiting a relatively smaller reduction in R_2* exhibited a greater increase in R_1. This suggests an oxygenated tumour region with saturated haemoglobin, which therefore exhibited greater blood O_2 concentration during carbogen breathing. Conversely, tumour regions which exhibited relatively large reductions in R_2* showed a less pronounced increase in R_1, consistent with a hypoxic yet erythrocyte perfused tumour region in which the deoxyhaemoglobin binds any dissolved molecular O_2 in the blood.

Conclusions: In a controlled preclinical setting, the GH3 tumour model exhibits a significant and positive ΔR_1 and significantly negative ΔR_2* during carbogen breathing. Large negative ΔR_2* and small ΔR_1 may indicate hypoxic tumour tissue, whereas small negative ΔR_2* and large ΔR_1 suggest oxygenated tumour regions. The combined use of ΔR_2* and ΔR_1 may prove more informative for the assessment of tumour hypoxia.

Acknowledgements: : This work was supported by BBSRC, AstraZeneca, The Royal Society, Cancer Research UK grant number C1060/A5117 and also NHS funding to the NIHR Biomedical Research Centre. We acknowledge the support received from the CRUK and EPSRC Cancer Imaging Centre in association with the MRC and Department of Health (England) grant C1060/A10334, also NHS funding to the NIHR Biomedical Research Centre

References: 1.) Tatum, J.L. et al., Int J Radiat Biol, 2006. **82**(10): p. 699-757.**2)**.Mirhej, M. CJC, 1964. **43**: p. 1130-1138.**3)**.O'Connor, J.P. et al., Mag Res Med, 2007. **58**(3): p. 490-6. **4)**.O'Connor, J.P. et al., Int J Radiat Oncol Biol Phys, 2009. **75**(4): p. 1209-15. **5)**.McPhail, L. and S. Robinson, Radiology, 2009: p. in press. **6)**.Alonzi, R., et al.Br J Cancer, 2009. **7)**.Robinson, S.P., et al. J Magn Reson Imaging, 2003. **17**(4): p. 445-54.**8)**.Landuyt, W., et al. J Magn Reson Imaging, 2002. **16**(2): p. 224-7. **9)**.Walker-Samuel, S. in *ISMRM Cancer Workshop*. 2008. Nice.